Article

Study of N$_2$O Formation over Rh- and Pt-Based LNT Catalysts

Lukasz Kubiak [1], Roberto Matarrese [1], Lidia Castoldi [1], Luca Lietti [1,*], Marco Daturi [2] and Pio Forzatti [1,*]

[1] Laboratory of Catalysis and Catalytic Processes, Dipartimento di Energia, Politecnico di Milano, Via La Masa, 34, 20156 Milano, Italy; lukaszmaciej.kubiak@polimi.it (L.K.); roberto.matarrese@polimi.it (R.M.); lidia.castoldi@polimi.it (L.C.)

[2] Laboratoire Catalyse et Spectrochimie, ENSICAEN, Université de Caen, CNRS, 6 Bd du Maréchal Juin, 14050 Caen, France; Marco.daturi@ensicaen.fr

* Correspondence: pio.forzatti@polimi.it (P.F.); luca.lietti@polimi.it (L.L.); Tel.: +3902-2399-3238 (P.F.); +3902-2399-3272 (L.L.)

Abstract: In this paper, mechanistic aspects involved in the formation of N$_2$O over Pt-BaO/Al$_2$O$_3$ and Rh-BaO/Al$_2$O$_3$ model NO$_x$ Storage-Reduction (NSR) catalysts are discussed. The reactivity of both gas-phase NO and stored nitrates was investigated by using H$_2$ and NH$_3$ as reductants. It was found that N$_2$O formation involves the presence of gas-phase NO, since no N$_2$O is observed upon the reduction of nitrates stored over both Pt- and Rh-BaO/Al$_2$O$_3$ catalyst samples. In particular, N$_2$O formation involves the coupling of undissociated NO molecules with N-adspecies formed upon NO dissociation onto reduced Platinum-Group-Metal (PGM) sites. Accordingly, N$_2$O formation is observed at low temperatures, when PGM sites start to be reduced, and disappears at high temperatures where PGM sites are fully reduced and complete NO dissociation takes place. Besides, N$_2$O formation is observed at lower temperatures with H$_2$ than with NH$_3$ in view of the higher reactivity of hydrogen in the reduction of the PGM sites and onto Pt-containing catalyst due to the higher reducibility of Pt *vs.* Rh.

Keywords: lean NO$_x$ trap; N$_2$O formation; NO$_x$ storage reduction; Pt-BaO/Al$_2$O$_3$; Rh-BaO/Al$_2$O$_3$

1. Introduction

The removal of NO$_x$ under lean conditions according to the NO$_x$ Storage-Reduction (NSR) technique is a viable approach for both diesel and lean gasoline fueled engines [1]. In this process NO$_x$ conversion is based on a cyclic engine operation alternating between fuel lean and rich conditions: NO$_x$ (NO+NO$_2$) are adsorbed on the catalyst surface during lean operations, while the surface of the trap is regenerated under the fuel rich environment. The NO$_x$ adsorption step involves oxidation sites (generally provided by noble metals like Pt, Pd or Rh) and alkali or alkaline-earth oxides storage sites (Ba, K, Sr), whereas the reduction stage involves reduction sites provided by the noble metals. All these components are deposited over a high surface area support like γ-Al$_2$O$_3$.

The operation of NSR catalysts (also known as Lean NO$_x$ Traps, LNTs) reduces NO$_x$ mainly to N$_2$ although undesired by-products like NH$_3$ or N$_2$O may also be generated. NH$_3$ is not generally a concern since an ammonia Selective Catalytic Reaction (SCR) catalyst can be placed downstream of the NSR system, such as in the case of combined NO$_x$ storage and NH$_3$-SCR catalytic systems [2]. At variance, N$_2$O is a highly undesired by-product in view of its very high global warming potential (nearly 300 times that of CO$_2$). Over fully formulated catalysts, it has been shown that N$_2$O formation

is apparent both upon switch from lean to rich mode but also during the alternation from rich to lean regime [3–8]. It has been suggested that N_2O formation at the lean to rich transition occurs at the regeneration front, upon reduction of the stored NO_x over not fully reduced Platinum-Group-Metal (PGM) sites. On the other hand, N_2O formation upon the rich to lean transition originates from reaction between residual surface NO_x with reductive species (like NCO, CO or NH_3) in an adsorbed state [3,4,7]. This N_2O peak can be reduced if a neutral or slightly lean phase is inserted between the rich and the lean phase, since a more complete regeneration of the catalyst can be attained [9].

In order to provide further insights on the pathway involved in N_2O formation, a fundamental study was carried out on a model Pt-BaO/Al_2O_3 catalyst under simplified and controlled reaction conditions [10]. Accordingly the reactivity of gaseous NO alone and in the presence of various reducing agents like H_2, NH_3, and CO was analyzed by micro-reactor transient reactivity experiments and *operando* Fourier transform infrared (FT-IR) spectroscopy, to provide a complementary overview on the pathway of N_2O evolution. It has been shown that N_2O is formed from gaseous NO provided that a proper oxidation degree of the Pt sites is attained [10]. Accordingly the N_2O evolution was observed only in a narrow temperature range corresponding to the PtO to Pt transformation, determined by the reactivity of the reducing agents (H_2 > NH_3 > CO).

In this study the investigation previously carried out over the model Pt-BaO/Al_2O_3 sample has been extended to a Rh-containing sample. Since Rh is generally considered to play an important role in the reduction of NO_x [11], it is of interest to analyze the role of this component in the pathways involved in N_2O formation. For this purpose the reduction of gaseous NO in the presence of various reductants (H_2, NH_3) was investigated by transient microreactor experiments and *operando* FT-IR spectroscopy to combine gas-phase data with surface species analysis. To point out the role of NO_x surface species (nitrates) in the formation of N_2O, experiments were also performed with the same reductants after adsorption of NO_x on the catalyst surface.

2. Results and Discussion

2.1. NO-Temperature Programmed Reaction (NO-TPR)

The reactivity of NO over the reduced Pt-BaO/Al_2O_3 and Rh-BaO/Al_2O_3 was investigated at first. The results of the gas phase analysis are shown in Figure 1A,B for the Rh-BaO/Al_2O_3 and Pt-BaO/Al_2O_3 catalyst, respectively. In both cases a NO consumption peak is observed, with a minimum in NO concentration centered near 250 and 200 °C for Rh-BaO/Al_2O_3 and Pt-BaO/Al_2O_3, respectively. The NO consumption is more evident in the case of the Pt-BaO/Al_2O_3 catalyst sample; in both cases it is accompanied by evolution of N_2O and of minor amounts of N_2. Notably, the NO consumption is not balanced by the evolution of N_2O (and of N_2), indicating the build up of N-containing species on the catalyst surface.

The results of surface analysis are shown in Figure 2. In the case of Rh-BaO/Al_2O_3 catalyst (Figure 2A) upon exposure of NO at 50 °C (spectrum a) a band appears at 1210 cm^{-1} corresponding to $\nu_{asym}(NO_2)$ vibration of chelating nitrites on the barium phase. The presence of the $\nu_{sym}(NO_2)$ mode of nitrites may also be observed near 1365 cm^{-1}. Upon heating, the band located at 1210 cm^{-1} increases, reaches a maximum intensity around 200–250 °C (spectra e–g) and then decreases with temperature. The decrease of the bands of nitrites is accompanied by an increase in the bands located near 1327 and 1405 cm^{-1} associated with ionic nitrates ($\nu_{asym}(NO_3)$ at 1327 and 1405 cm^{-1}). The presence of an isosbestic point suggests the occurrence of the transformation of nitrites into nitrates on the catalyst surface. The appearance of nitrate species is also confirmed by the presence of a low intensity peak at 1030 cm^{-1} ($\nu_{sym}(NO_3)$). Furthermore, a shoulder near 1545 cm^{-1}, associated with bidentate nitrates (ν(N=O)) is also detected. At the end of the temperature ramp (350 °C) the surface of the catalyst is dominated by the presence of nitrate species, however nitrites are still present (band at 1210 cm^{-1}).
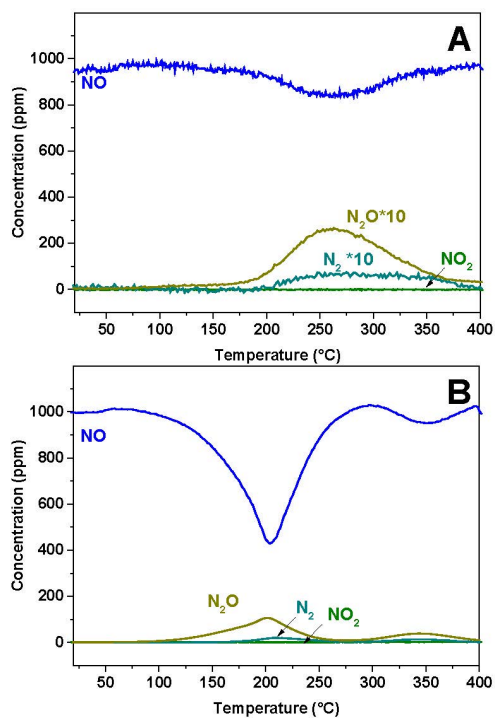
Figure 1. NO-TPR experiments with NO (1000 ppm) in He from 40–400 °C (10 °C/min) over pre-reduced Rh-BaO/Al$_2$O$_3$ (**A**) and Pt-BaO/Al$_2$O$_3$ (**B**) catalysts (rig #1).
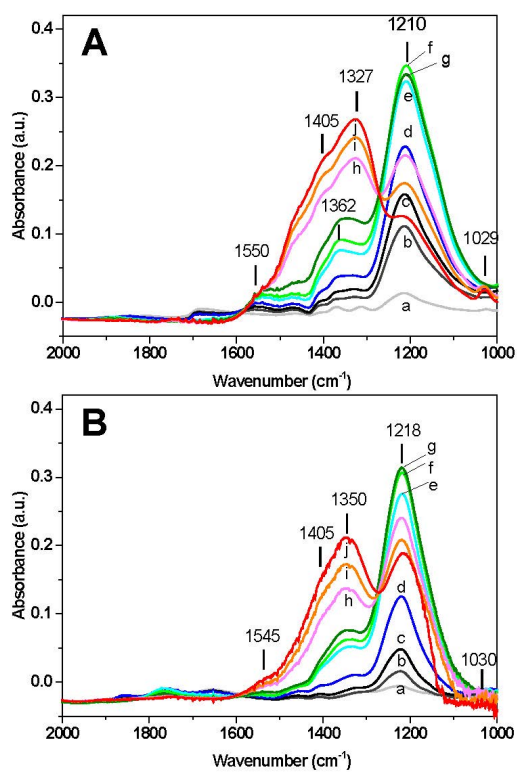

Figure 2. Operando FT-IR spectra recorded during NO-TPR experiments with NO (1000 ppm) in He over Rh-BaO/Al$_2$O$_3$ (**A**) and Pt-BaO/Al$_2$O$_3$ (**B**) from 50 to 350 °C (10 °C/min), spectra recorded every 1 min, displayed at selected temperatures: (**a**) 50 °C; (**b**) 100 °C; (**c**) 120 °C; (**d**) 150 °C; (**e**) 200 °C; (**f**) 220 °C; (**g**) 250 °C; (**h**) 300 °C; (**i**) 320 °C; (**l**) 350 °C (rig#2).
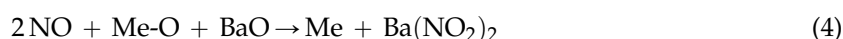
A similar picture was observed over the Pt-BaO/Al$_2$O$_3$ catalyst (Figure 2B), with only minor differences. Also in this case the formation of chelating nitrites (1218 cm^{-1}) is seen at the initial stage, reaching a maximum in the same temperature range (220–250 °C) observed for the Rh-based catalyst. Then the bands decrease in favor of nitrate formation, as pointed out by the isosbestic point and by the growth of the bands near 1350 and 1405 cm^{-1}. At the end of the run (350 °C), the final amount of nitrites on the Pt containing catalyst is higher if compared to the Rh-based sample, as pointed out by the relative intensity of the bands at 1218 cm^{-1} (nitrites) and at 1350–1405 cm^{-1} (nitrates).

The above results clearly show that upon contacting NO with the reduced catalyst surface, NO is consumed leading to N$_2$O and nitrites adsorbed over the barium surface. In particular the results are in line with the occurrence, below 250 °C, of the following NO disproportion reaction Equation (1):

$$4\,NO\,+\,BaO \rightarrow N_2O\,+\,Ba(NO_2)_2 \tag{1}$$
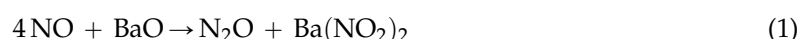
In fact the ratio between NO consumption and N$_2$O formation is not very far from the theoretical value 1:4 expected from the stoichiometry of the overall reaction Equation (1). At higher temperature, above 250 °C, nitrites are transformed into nitrates, in line with previous results [10].

The overall stoichiometry of the NO disproportion reaction Equation (1) can be explained by considering the occurrence of the following reactions Equations (2)–(4):

$$NO\,+\,2\,Me \rightarrow Me\text{-}N\,+\,Me\text{-}O \tag{2}$$

$$NO\,+\,Me\text{-}N \rightarrow N_2O\,+\,Me \tag{3}$$

$$2\,NO\,+\,Me\text{-}O\,+\,BaO \rightarrow Me\,+\,Ba(NO_2)_2 \tag{4}$$

where Me is the metal site (Pt or Rh). According to this scheme, the reaction is initiated at low temperature by the decomposition of NO over reduced Me sites, leading to the formation of N- and O-adspecies (reaction Equation (2)). The formation of oxidized metal sites (Me-O species) prevents the dissociation of other NO molecules and this results in the formation of N$_2$O (reaction Equation (3)) and of nitrites on Ba (reaction 4)). The occurrence of reaction Equation (4) removes O-adatoms on metal sites leaving vacant metal sites accessible for further NO dissociation. Reactions Equations (2)–(4) lead to the overall stoichiometry of reaction Equation (1).

Worth noting is that reactions Equations (2)–(4) require the presence of reduced metal sites, to initiate the NO dissociation reaction. In fact the NO disproportion reaction is observed to a much lower extent over an oxidized Pt-based catalyst sample (data not reported). Along similar lines, the storage component BaO is also important in that it provides the adsorption sites for the nitrite (and nitrate) surface species. In fact, experiments carried out over a bare Pt/Al$_2$O$_3$ sample pointed out a much lower N$_2$O (and nitrite) formation. However, the presence of BaO may also increase the activity of the metal sites in the dissociative chemisorption of NO, as reported elsewhere [12].

2.2. NO/H$_2$-TPR

To investigate the effect of the presence of a reductant in N$_2$O formation, experiments were carried out in the presence of H$_2$ and results are shown in Figure 3A,B in the case of Rh-BaO/Al$_2$O$_3$ and Pt-BaO/Al$_2$O$_3$ catalysts, respectively.

In the case of the Rh-based catalyst, NO starts to be converted near 150 °C, with formation of N$_2$O and N$_2$ in nearly equal amounts. Then, above 200 °C, NO is fully consumed and N$_2$O formation rapidly drops. Accordingly above 200 °C only N$_2$ and NH$_3$ are seen in the reaction products.

Very similar results are observed in the case of the Pt-BaO/Al$_2$O$_3$ catalyst (Figure 3B). However, in this case NO consumption is observed at much lower temperatures (onset temperature near 50 °C), and the NH$_3$ selectivity at high temperatures is much higher if compared to the Rh-BaO/Al$_2$O$_3$ sample.
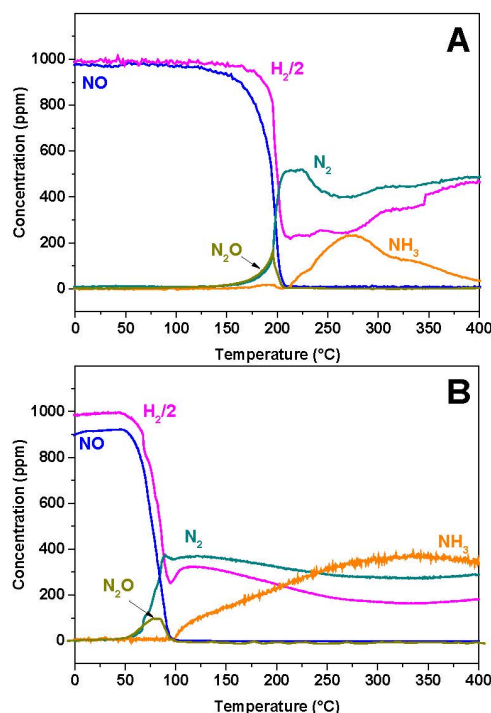
Figure 3. NO/H_2-TPR experiments with NO (1000 ppm) + H_2 (2000 ppm) over (**A**) Rh-BaO/Al_2O_3 and (**B**) Pt-BaO/Al_2O_3 from 40–400 °C (4 °C/min), (rig#3).

The correspondent surface analysis is shown for the Pt-BaO/Al_2O_3 sample in Figure 4. Upon NO admission, the formation of a very weak band at 1218 cm^{-1} is seen, related to the formation of chelating nitrites on the Ba phase. This band slightly increases with temperature, reaches a weak maximum near 85 °C and then disappears at higher temperatures, along with N_2O. The spectra also show complex bands in the range 1300–1600 cm^{-1}, with positive and negative contributions. These bands are related to modifications of a covalent carbonate species, initially present on the surface, into more symmetric, ionic species upon interaction with water formed during the reduction of NO with H_2 and upon the temperature increase.
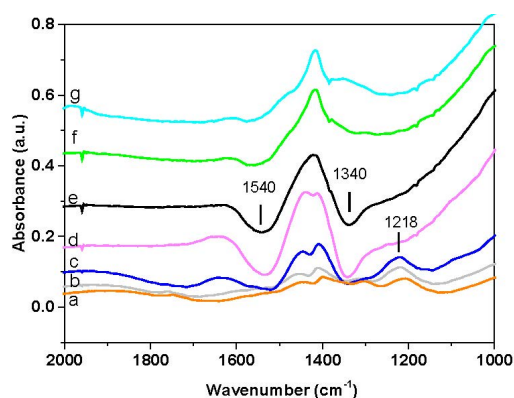

Figure 4. FT-IR spectra obtained during NO/H_2–TPR with NO (1000 ppm) + H_2 (2000 ppm) over Pt-BaO/Al_2O_3 from 40–400 °C (4 °C/min) at: (**a**) 40 °C; (**b**) 77 °C; (**c**) 85 °C; (**d**) 152 °C; (**e**) 252 °C; (**f**) 354 °C; (**g**) 400 °C (rig#3).

Very similar results were obtained in the case of the Rh-based sample (not shown): also in this case we observed the formation of a weak nitrite band in the temperature range where N_2O is formed.

Upon comparing these results with those obtained in the absence of H_2 (*i.e.*, the NO-TPR runs, Figures 1 and 2), it clearly appears that N_2O formation is seen at much lower temperatures in the case of the Pt-BaO/Al_2O_3 sample, and at slightly higher temperatures in the case of the Rh-based sample. In both cases N_2O formation is accompanied by nitrite evolution, although the band of nitrites is much lower in the presence of H_2.

As suggested above (see reactions Equations (2)–(4)), N_2O (and nitrite) formation requires the presence of reduced Me (Pt, Rh) sites. Hence the reaction is initiated by the reduction of the PGM sites by H_2: the lower onset temperature for NO reduction illustrates the much higher reducibility of the Pt-based sample if compared to the Rh-BaO/Al_2O_3 catalyst.

As shown in Figure 3, the NO reduction reaction leads at low temperatures to the formation of N_2 and N_2O. Then, at higher temperatures, N_2O formation becomes nil and the selectivity shifts towards N_2 and NH_3. It is speculated that upon reduction of the PGM sites by H_2, N_2O (and nitrite) formation occurs according to reactions Equations (2)–(4). The presence of H_2 leads also to the formation of Rh-H and Pt-H species, according to the reaction Equation (5).

$$H_2 \, + \, 2\,Me \rightarrow 2\,M\text{-}H \tag{5}$$

where Me is the metal site (Pt or Rh). The so formed Me-H species scavenge O-adatoms, reaction Equation (6):

$$2\,Me\text{-}H \, + \, Me\text{-}O \rightarrow 3\,Me \, + \, H_2O \tag{6}$$

The scavenging of O-adatoms according to reaction Equation (6) limits the formation of nitrites according to reaction Equation (4), as indeed is observed in the presence of H_2.

Besides, N_2 formation is also observed along with N_2O, coming from the coupling of N-adatoms (reactions Equations (2) and (7)):

$$2\,Me\text{-}N \rightarrow 2\,Me \, + \, N_2 \tag{7}$$

Since the O-removal efficiency by H_2 increases with temperature, upon increasing the temperature NO completely dissociates and N-adatoms lead to the formation of N_2 (reaction Equation (7)) or of NH_3 (reaction Equation (8)), thus shifting the selectivity towards N_2 and NH_3:

$$M\text{-}N \, + \, 3\,M\text{-}H \rightarrow 4\,M \, + \, NH_3 \tag{8}$$

Notably, in the case of the Rh-containing catalyst, the NH_3 concentration decreases above 275 °C. This is due to the occurrence of the NH_3 decomposition reaction, which is efficiently catalyzed over Rh, as it is shown below.

2.3. NO/NH$_3$-TPR

Figure 5 shows the results obtained during the reduction of NO with NH_3 in the case of Rh-BaO/Al_2O_3 (Figure 5A) and Pt-BaO/Al_2O_3 catalysts (Figure 5B). The onset temperature for NO reduction is seen near 200 and 100 °C for the Rh- and Pt-based catalysts, respectively. These temperature thresholds are higher than those measured in the case of H_2, but show the same order of reactivity of the investigated samples, being the Pt-BaO/Al_2O_3 catalyst more reactive than Rh-BaO/Al_2O_3. Over both the catalytic systems the initial formation of N_2O and N_2 is observed; then, when complete NO consumption is attained (*i.e.*, near 295 °C and 185 °C over Rh-BaO/Al_2O_3 and Pt-BaO/Al_2O_3, respectively) the N_2O concentration drops to zero resulting in complete N_2 selectivity. In the case of the Rh-based sample, above 300 °C an increase in the N_2 concentration is observed, along with H_2 and a correspondent decrease of the NH_3 concentration. This is due to the occurrence of the NH_3 decomposition reaction:

$$2\,NH_3 \rightarrow N_2 \, + \, 3\,H_2 \tag{9}$$

which is catalyzed by the Rh component.
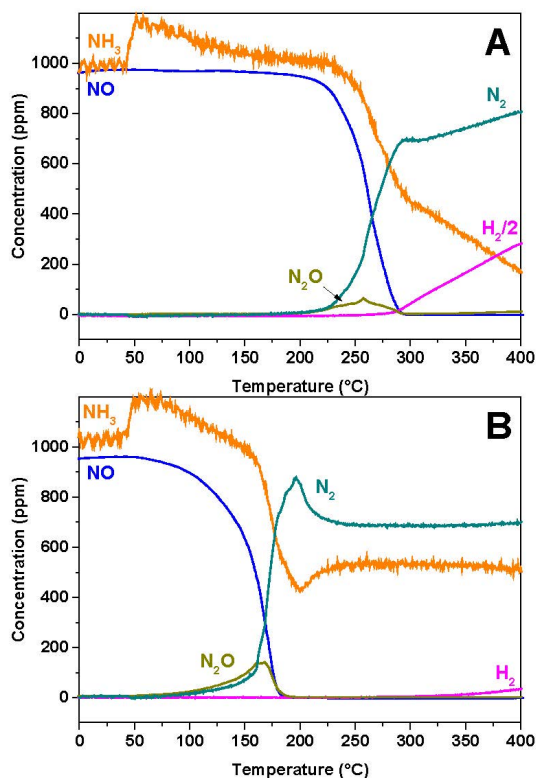
Figure 5. NO/NH$_3$-TPR experiments with NO (1000 ppm) + NH$_3$ (1000 ppm) over (**A**) Rh-BaO/Al$_2$O$_3$ and (**B**) Pt-BaO/Al$_2$O$_3$ from 40–400 °C (4 °C/min) (rig#3).

The results of the FT-IR analysis carried out over the Rh-BaO/Al$_2$O$_3$ and the Pt-BaO/Al$_2$O$_3$ catalysts are shown in Figure 6A,B respectively. In the case of Rh-BaO/Al$_2$O$_3$ (see Figure 6A), upon NH$_3$ admission, bands at 1095 and 1647 cm^{-1} (low intensity) immediately appear (spectrum a). These bands are related to the symmetric and antisymmetric bending modes of ammonia. Then, upon NO admission, a weak band of nitrites appears at 1212 cm^{-1}. Upon heating, the bands associated with NH$_3$ decrease and eventually disappear. Besides, the nitrite band slightly increases up to 275 °C and then disappears. In addition to these bands, positive and negative bands are evident in the spectra due to the distortion of carbonate species, as previously discussed.

The Pt-BaO/Al$_2$O$_3$ catalyst shows similar features (see Figure 6B) but a much higher amount of nitrites is formed upon NO admission, with respect to Rh-BaO/Al$_2$O$_3$. Nitrites readily disappear near 200 °C (spectrum g).

The picture obtained from the analysis with NH$_3$ is consistent with that discussed in the case of H$_2$. Upon reduction of the PGM sites by NH$_3$, NO is dissociated into N- and O-adatoms and formation of N$_2$O and nitrites is observed (reactions Equations (2)–(4)). Formation of these species is observed at lower temperatures over the Pt-based sample in view of its higher reactivity, in line with data obtained during the NO/H$_2$-TPR.

By comparing NO/NH$_3$-TPR and NO/H$_2$-TPR data, it is apparent that the onset of N$_2$O formation is shifted towards higher temperatures (compare Figures 3A and 4A) and also higher amounts of nitrites are formed. This can be explained considering that NH$_3$ is a much less efficient reductant (*i.e.*, a less efficient O-scavenger) compared to H$_2$. This results in a higher onset temperature for the reaction and a higher temperature for complete NO dissociation.
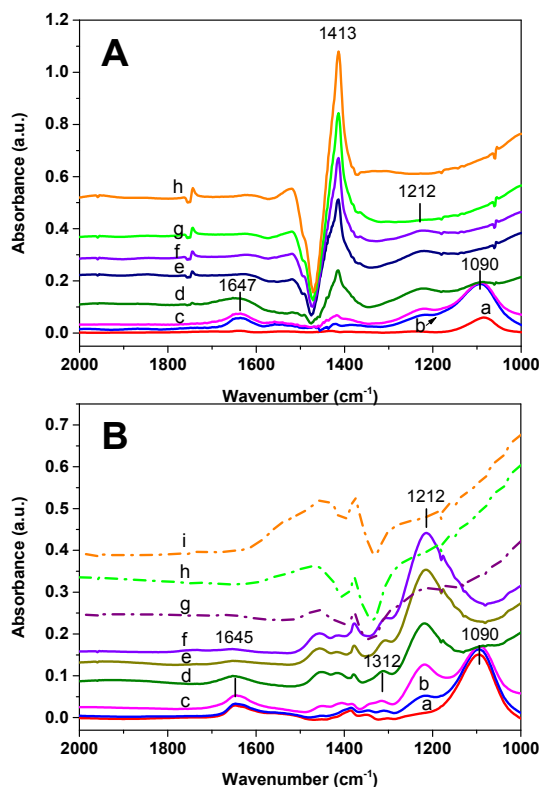
Figure 6. Operando FT-IR spectra during NO/NH_3–TPR with NO (1000 ppm) + NH_3 (1000 ppm) from 40–400 °C (4 °C/min) over (**A**) Rh-BaO/Al_2O_3 at: (**a**) 40 °C with NH_3; (**b**) 40 °C with NH_3+NO; (**c**) 40 °C before temperature ramp; (**d**) 50 °C; (**e**) 104 °C; (**f**) 260 °C; (**g**) 292 °C; (**h**) 400 °C. Panel (**B**) Pt-BaO/Al_2O_3 at: (**a**) 40 °C with only NH_3; (**b**) 40 °C NH_3 + NO; (**c**) 40 °C before temperature ramp; (**d**) 104 °C; (**e**) 153 °C; (**f**) 178 °C; (**g**) 203 °C; (**h**) 328 °C; (**i**) 400 °C (rig#3).

In the case of NO/NH_3-TPR experiments, N_2O and N_2 formation involves coupling of N-containing species coming from NO and/or NH_3 molecules. To investigate such aspects, isotopic labeling experiments were carried out with NH_3 and ^{15}NO over both Pt- [13] and Rh-BaO/Al_2O_3 [14]. In both cases the low-T NO consumption (*i.e.,* below the maximum in N_2O concentration) is accompanied by the evolution of double labeled $^{15}N_2O$ and of single labeled N_2 ($^{15}N^{14}N$), with only minor amounts of single labeled N_2O ($^{15}N^{14}NO$). Then, at higher temperatures (near the complete NO consumption) N_2O is no more detected among the reaction products and all the N_2 isotopes are observed.

These results indicate that N_2O formation involves primarily NO molecules only, according to reactions Equations (2) and (3). In this pathway, the role of NH_3 is hence that of keeping the noble metal sites in a reduced state, with formation of Me-H and Me-NH_2 species according to reaction Equation (10):

$$NH_3 + 2\,Me \rightarrow Me\text{-}NH_2 + Me\text{-}H \tag{10}$$

Me-H scavenges O-adatoms, resulting in H_2O formation while Me-NH_2 reacts with (labelled) nitrite species leading to the formation of the single labelled N_2 ($^{15}N^{14}N$), according to reaction Equation (11), where $O^=$ is lattice oxygen:

$$Me\text{-}NH_2 + {}^{15}NO_2 \rightarrow Me + {}^{15}N^{14}N + 3/2\,H_2O + \tfrac{1}{2}O^= \tag{11}$$
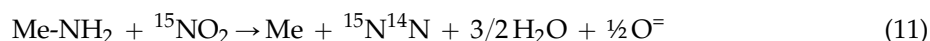
This accounts for the formation of single labelled N_2 that accompanies N_2O evolution. At higher temperatures, near complete NO consumption where no N_2O is seen, all N_2 isotopes are detected due to the statistical coupling of N-adatoms coming from NO- and NH_3-decomposition [13].

2.4. H_2-Temperature Programmed Surface Reaction (H_2-TPSR)

Figure 7 shows the results of the H_2-TPSR experiments performed over Rh-BaO/Al_2O_3 and Pt-BaO/Al_2O_3 after NO_x adsorption at 350 °C. The gas phase results are shown in Figure 7A,B for the Rh- and Pt-based catalyst samples, respectively. In the case of the Rh-containing sample, the temperature threshold for hydrogen consumption is seen near 170 °C. Above 200 °C NH_3 evolution is seen, followed by that of N_2 above 300 °C. The initial H_2 consumption is probably related to the reduction of the Rh sites, since it is not accompanied by the release of reaction products.
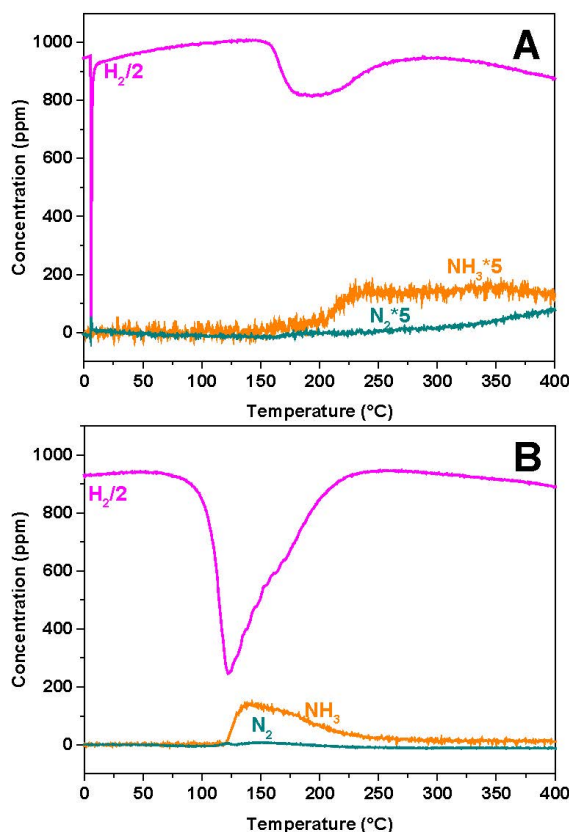

Figure 7. H_2-TPSR experiments with H_2 (2000 ppm) from 40–400 °C (4 °C/min) after NO/O_2 adsorption at 350 °C over (**A**) Rh-BaO/Al_2O_3 and (**B**) Pt-BaO/Al_2O_3 (rig#3).

The corresponding FT-IR spectra are shown in Figure 8A. The spectrum recorded prior to H_2 consumption (spectrum a) corresponds to the surface ionic nitrate ($\nu_{asym}(NO_3)$ mode split into two peaks at 1400 and 1330 cm^{-1}; $\nu_{sym}(NO_3)$ mode at 1035 cm^{-1}). The band near 1470 cm^{-1} is an artefact due to the presence of carbonate species, which have been partially displaced upon adsorption of NO_x and therefore lead to the formation of negative peaks in the subtraction spectra. Consequently, FT-IR analysis confirms that NO_x have been stored at 350 °C in the form of nitrate species.

Upon heating, the reduction of nitrates occurs from 200 °C, as it is obvious from the corresponding decrease of the bands. The nitrate bands decrease in intensity with temperature, and no new bands are apparent. At 388 °C (spectrum j) the surface is clean and only a negative band at 1440 cm^{-1} is visible, due to carbonates that have been displaced upon nitrate adsorption from NO/O_2 at 350 °C.

These results indicate that, over Rh-BaO/Al_2O_3, the stored nitrates are reduced by hydrogen selectively into NH_3 (and minor amounts of N_2), without any formation of NO or N_2O.
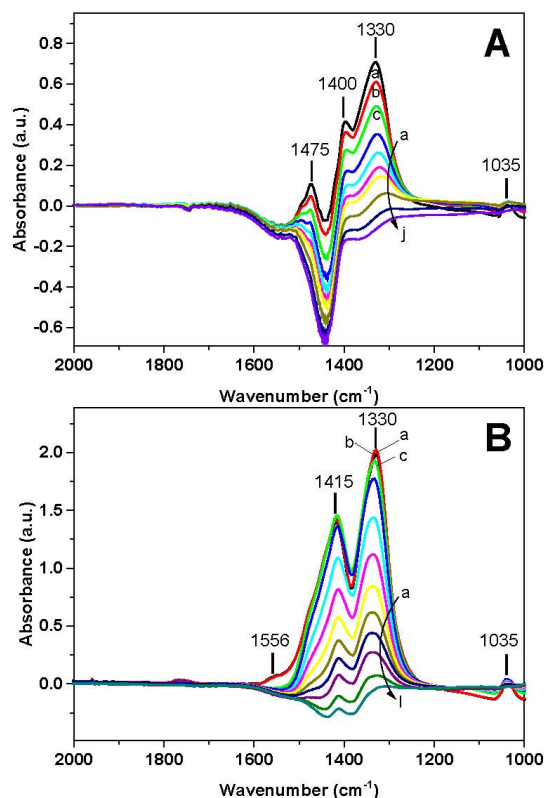
Figure 8. Operando FT-IR spectra obtained during H_2-TPSR experiments with H_2 (2000 ppm) from 40–400 °C (4 °C/min) after NO/O_2 adsorption at 350 °C over (**A**) Rh-BaO/Al_2O_3 at: (**a**) 157 °C; (**b**) 200 °C; (**c**) 215 °C; (**d**) 232 °C; (**e**) 248 °C; (**f**) 264 °C; (**g**) 281 °C; (**h**) 322 °C; (**i**) 355 °C; (**j**) 388 °C; and (**B**) Pt-BaO/Al_2O_3 at: (**a**) 40 °C; (**b**) 49 °C; (**c**) 107 °C; (**d**) 115 °C; (**e**) 124 °C; (**f**) 132 °C; (**g**) 140 °C; (**h**) 148 °C; (**i**) 157 °C; (**j**) 165 °C; (**k**) 182 °C; (**l**) 198 °C (rig#3).

Similar results were obtained in the case of the Pt-containing catalyst (Figures 7B and 8B). Gas phase analysis (Figure 7B) shows that H_2 consumption is seen starting from 100 °C, *i.e.*, at lower temperatures than Rh-BaO/Al_2O_3. The H_2 consumption is accompanied by the formation of ammonia with traces of nitrogen; no other reaction products (e.g., NO, N_2O) are formed. Also in this case the H_2 consumption is seen before the evolution of the reaction products, likely indicating the reduction of the catalyst metal sites.

Surface analysis (Figure 8B) showed the presence of the ionic nitrates (ν_{asym} (NO_3)) mode split into two peaks at 1417 and 1320 cm^{-1}; $\nu_{sym}(NO_3)$ mode at 1035 cm^{-1}) and minor amounts of bidentate nitrates ($\nu(N=O)$ mode at 1555 cm^{-1}) on the catalyst surface at the beginning of the run (spectrum a). The reduction of nitrates is observed above 115 °C, in line with gas-phase results. Upon increasing the temperature the reduction of nitrates proceeds faster and complete reduction is attained above 200 °C, at a much lower temperature with respect to Rh-BaO/Al_2O_3. Also in this case, residual carbonates, present on the surface before the NO_x storage, were removed and this results in weak negative bands at 1440 and 1380 cm^{-1}.

H_2-TPSR experiments hence indicate that the reduction with H_2 of nitrates stored over both Pt- and Rh-containing catalyst samples does not lead to the formation of N_2O. The Pt-BaO/Al_2O_3 sample is more active than the Rh-containing catalyst but in both cases only NH_3 was observed as reduction product, along with traces of N_2. These results are in line with previous data obtained over the same Pt-containing sample used in this study and published elsewhere [15].

2.5. NH$_3$–TPSR

Figures 9 and 10 show the results obtained during TPSR experiments performed with NH$_3$ after NO$_x$ adsorption at 350 °C. The gas phase results are shown in Figure 9A,B for Rh-BaO/Al$_2$O$_3$ and Pt-BaO/Al$_2$O$_3$, respectively. In the case of the Rh-catalyst (Figure 9A), ammonia desorption is observed at the beginning of the heating ramp. Then the temperature onset for ammonia consumption is seen near 250 °C, *i.e.*, at higher temperatures if compared to H$_2$ (see Figure 7A). The NH$_3$ consumption is accompanied by the formation of nitrogen, whose concentration shows a peak with maximum near 280 °C. At temperatures above 300 °C ammonia is further consumed leading to the evolution of N$_2$ and H$_2$. The initial N$_2$ formation, with maximum near 280 °C, is due to the reduction of the stored nitrates, whereas the nitrogen formation above 300 °C is due to occurrence of the NH$_3$ decomposition reaction. Notably, the reduction of the stored nitrates with ammonia is fully selective to N$_2$, and neither N$_2$O nor NO formation was observed.
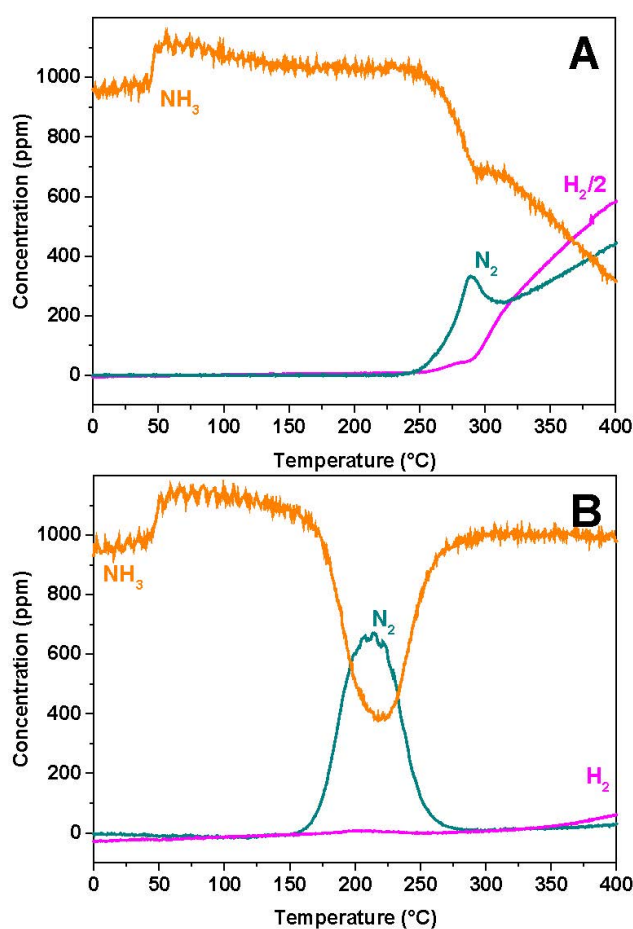

Figure 9. NH$_3$-TPSR experiments with NH$_3$ (1000 ppm) from 40–400 °C (4 °C/min) after NO/O$_2$ adsorption at 350 °C over: (**A**) Rh-BaO/Al$_2$O$_3$ and (**B**) Pt-BaO/Al$_2$O$_3$ (rig#3).

FT-IR spectra recorded during the NH$_3$-TPSR are shown in Figure 10A. Ionic nitrates (bands at 1402, 1338, and 1036 cm^{-1}) and adsorbed ammonia (bands at 1095 and 1640 cm^{-1}) are initially present on the catalyst surface at 40 °C (spectrum a). The increase of the temperature leads at first to the disappearance of the 1095 and 1640 cm^{-1} bands, in line with the desorption of NH$_3$ (spectrum b). At further temperature increase, nitrates are reduced and at 400 °C (spectrum i) the surface is free from nitrates.
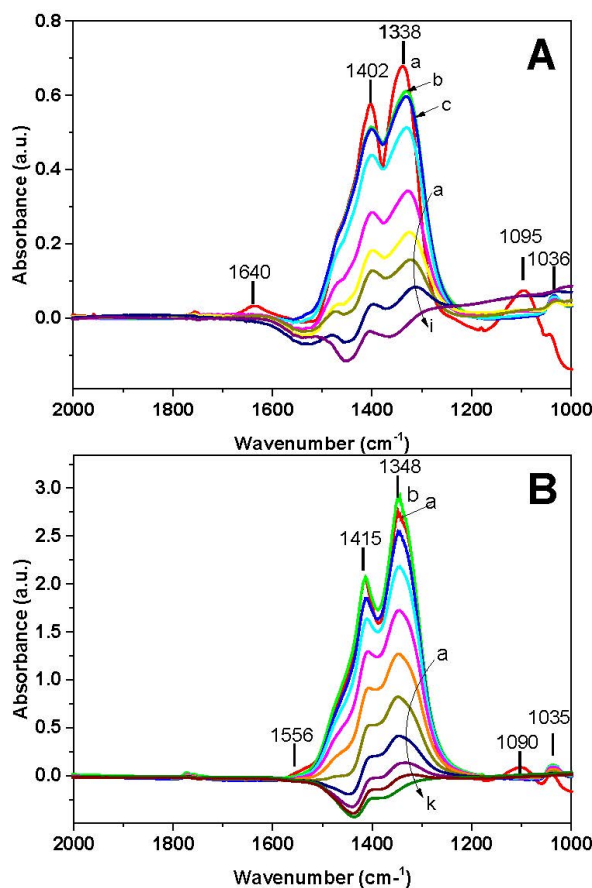
Figure 10. Operando FT-IR spectra obtained during NH_3-TPSR experiments with NH_3 (1000 ppm) from 40–400 °C (4 °C/min) after NO/O_2 adsorption at 350 °C over (**A**) Rh-BaO/Al_2O_3 at: (**a**) 40 °C; (**b**) 275 °C; (**c**) 283 °C; (**d**) 291 °C; (**e**) 300 °C; (**f**) 308 °C; (**g**) 316 °C; (**h**) 333 °C; (**i**) 400 °C; and (**B**) Pt-BaO/Al_2O_3 at: (**a**) 40 °C; (**b**) 171 °C; (**c**) 196 °C; (**d**) 204 °C; (**e**) 213 °C; (**f**) 221 °C; (**g**) 229 °C; (**h**) 237 °C; (**i**) 246 °C; (**j**) 254 °C; (**k**) 303 °C (rig#3).

In the case of the Pt-catalyst (Figure 9B), the temperature threshold for ammonia consumption is observed near 150 °C, *i.e.*, at lower temperatures if compared to the Rh-containing sample, and leads to N_2 formation with a maximum near 220 °C. At 270 °C nitrogen evolution is completed and the NH_3 concentration reaches the inlet concentration value. Also in this case the reaction is fully selective towards nitrogen, and no N_2O formation was observed. Above 350 °C the Pt-catalyst shows a limited activity in the dissociation of NH_3, as pointed out by the small evolution of H_2 and of nitrogen. Concerning the surface phase (Figure 10B), ionic nitrates (bands at 1415, 1348, and 1035 cm^{-1}), bidentate nitrates (1555 cm^{-1}) and adsorbed ammonia (band at 1090 cm^{-1}) are initially present (40 °C, spectrum a). Upon increasing the temperature, initially bidentate nitrates are transformed into ionic nitrates (spectrum b) and then ionic nitrates decrease. Above 250 °C nitrates are completely removed (spectra j and k).

The results hence indicate that over both catalyst samples NH_3 is an effective reductant for the stored nitrates, although it is less efficient than H_2. The Pt-containing sample is more reactive than the Rh-based catalyst. Notably, no N_2O is formed upon the reduction of the stored nitrates, the reaction being very selective towards N_2. This apparently rules out the involvement of surface nitrates and/or nitrate containing compounds (e.g., ammonium nitrate) in the formation of N_2O, at least under the investigated experimental conditions.

3. Pathways for N$_2$O Formation

The results of the reactivity of gas-phase NO and adsorbed NO$_x$ species with H$_2$ and NH$_3$ clearly illustrated that N$_2$O is formed only during the run with the presence of gas-phase NO. In fact no nitrous oxide formation has been observed both over the Pt- and Rh-BaO/Al$_2$O$_3$ catalysts upon the reduction of stored nitrates, where no gas-phase NO is fed to the catalyst samples.

Notably, N$_2$O is formed even in the absence of reductants (*i.e.*, from NO alone), provided that reduced PGM sites are present over the catalyst surface. Reduced Pt or Rh sites catalyze the NO dissociation reaction into N- and O-adatoms; N-species further interact with undissociated NO molecules (either in the gas-phase or from an adsorbed state) leading to the formation of N$_2$O. This pathway is represented by reactions Equations (2) and (3) previously discussed.

In the absence of any reductant, the reaction is self-inhibited by the formation of oxidized PGM sites (*i.e.*, O-adatoms), formed upon NO dissociation. In this respect, NO itself acts as a weak reductant, being able to scavenge O-adatoms and resulting in the formation of nitrite species adsorbed over the storage component (Ba). The overall stoichiometry of the process is then well described by following NO disproportion reaction Equation (1).

Hence also the storage element participates in the reaction, providing the adsorption sites for nitrites. It may also increase the reactivity of the PGM sites in the NO dissociative chemisorption, as suggested in the literature [10,12]. In fact, experiments carried out over a Ba-free sample showed a much lower N$_2$O formation if compared to the Ba-containing catalysts [14].

Reduced Pt- and Rh-based catalysts show similar reactivity in the N$_2$O formation from NO, N$_2$O being formed at the same temperature, although in the case of the Rh-containing catalyst much lower amounts of N$_2$O were detected. This is likely related to the lower metal dispersion of the Rh-BaO/Al$_2$O$_3$ catalyst if compared to the Pt-containing sample (6.8% *vs.* 48%, see Table 1), and hence to the lower amounts of surface reduced sites.

Table 1. Morphological characterization of catalysts.

Catalyst	Surface Area, m^2/g	Pore Volume, cm^3/g	Pore Radius, Å	Metal Dispersion, %
Pt-BaO/Al$_2$O$_3$	133	0.63	93	48
Rh-BaO/Al$_2$O$_3$	150	0.76	102	6.8

When a reductant (H$_2$ or NH$_3$) is co-fed with NO, N$_2$O always appears as the first NO reduction product, along with nitrogen. The onset temperature for NO reduction (and N$_2$O evolution) depends on the nature of the reductant (with H$_2$ showing a greater reactivity than NH$_3$) and on the catalyst as well (Pt-based catalyst being more active than the corresponding Rh-containing sample). The pathways involved in N$_2$O formation are those already depicted for NO alone: the reductant leads to the reduction of the PGM sites, leading to NO dissociation into N- and O-adatoms. However in this case O-adatoms are scavenged by the reductant, and nitrite formation is reduced with respect to the reaction of pure NO. When the reactivity of the reductant is not very high (*i.e.,* near the onset temperature for NO reduction) the PGM sites are not fully reduced and hence there is the chance for N-adspecies to react with undissociated NO molecules, leading to N$_2$O evolution. At variance, when the reductant maintains the PGM sites in a fully reduced state, NO is readily dissociated and the reduction products are N$_2$ and NH$_3$ (when H$_2$ is used as reductant) or N$_2$ (reductant NH$_3$). It is concluded that the formation of N$_2$O occurs only in the presence of undissociated NO molecules, *i.e.,* when the PGM sites are not fully reduced. Accordingly, the temperature onset for N$_2$O formation depends on the reactivity of the reductant: it is seen at lower temperature when H$_2$ is used as a reductant instead of NH$_3$, due to the higher reactivity of H$_2$.

Notably, no N$_2$O formation was observed under our experimental conditions upon reduction with both H$_2$ and NH$_3$ of nitrates stored over both Pt- and Rh-BaO/Al$_2$O$_3$. Notably, the intermediacy of species like ammonium nitrate in N$_2$O formation is apparently ruled out since no N$_2$O was observed

in the NH_3/nitrate reaction over both Pt- and Rh-based catalytic materials. It has been suggested that the reduction of the stored NO_x species is involved in the release of NO from the stored NO_x as first step, followed by the reduction of the released NO over the PGM sites [16–19]. The reduction process is initiated by the reduction of the PGM sites by the reductant, which precedes the NO release. The observation that no N_2O is formed in this case may be explained by considering that the rate determining step in the reduction of the stored NO_x is the NO release step [16]; once NO is released, it is readily converted to the reduction products. Accordingly the gas-phase concentration of NO is small and this prevents N_2O formation. However under real operating conditions, where significant temperature effects may take place, significant release of NO may take place and accordingly N_2O formation is likely to occur.

4. Materials and Methods

Model Pt-BaO/Al$_2$O$_3$ (1/20/100 *w/w/w*) and Rh-BaO/Al$_2$O$_3$ (0.5/20/100 *w/w/w*) samples were prepared by incipient wetness impregnation of a commercial γ-alumina (Versal 250 UOP, Des Plaines, IL, USA) support with Pt(NO$_2$)$_2$(NH$_3$)$_2$ (Strem Chemicals, 5% *w/w*, Newburyport, MA, USA) and Rh(NO$_3$)$_3$ (Sigma Aldrich, 10% *w/w*, St. Louis, MO, USA) aqueous solutions, respectively, followed by impregnation with Ba(CH$_3$COO)$_2$ (Sigma Aldrich, 99% *w/w*) aqueous solution. After each impregnation step the samples were dried at 80 °C overnight and calcined at 500 °C for 5 h. The obtained catalysts were characterized by Brunauer-Emmett-Teller (BET) analysis for specific surface area and H$_2$ chemisorption for metal dispersion and results are reported in Table 1.

The reactivity of NO alone and with different reductants (H$_2$, NH$_3$) was investigated *via* temperature programmed reaction (TPR) experiments. In the case of NO alone, the catalysts were heated in the temperature range 40–400 °C (heating rate 10 °C/min) under a flow of NO (1000 ppm in He, NO-TPR). Before performing the experiments, the catalysts were reduced with H$_2$ (2000 ppm in He) at 350 °C for 30 min and cooled to 40 °C in He. Such experiments were carried out in a flow micro-reactor apparatus consisting of an home made quartz tube reactor (7 mm I.D.) connected to a mass spectrometer (Omnistar 200, Pfeiffer Vacuum, Asslar, Germany), a micro-gas chromatograph (Agilent 3000A, Santa Clara, CA, USA) and a ultraviolet (UV) analyzer (Limas 11HW, ABB, Zurich, Switzerland) for the on-line analysis of the outlet gases (rig #1). An amount of 60 mg of catalyst was used with a flow rate of 100 cc/min (at 0 °C and 1 atm).

Information on the surface species formed during the experiments was collected in this case by performing the NO-TPR experiments under the same experimental conditions inside an IR reactor cell (ISRI Infrared Reactor, Granger, IN, USA) by using the catalysts in form of self-supported wafers (15 mg, diameter = 13 mm, thickness = 0.1 mm) (rig #2). The IR measurements were collected with a FT-IR Vertex 70 (Bruker, Billerica, MA, USA) spectrometer with 4 cm^{-1} spectral resolution and accumulation of 64 scans using a mercury-cadmium-telluride (MCT) detector.

The reactivity of NO with H$_2$ and NH$_3$ (NO/H$_2$-TPR and NO/NH$_3$-TPR, respectively) was investigated by heating the catalyst samples in a flow of NO (1000 ppm) with H$_2$ (2000 ppm) or NH$_3$ (1000 ppm) in Ar in the temperature range 40–400 °C (heating rate 4 °C/min). These experiments were carried out in an *operando* FT-IR spectroscopy setup (rig #3) consisting in a "Sandwich" IR cell containing the catalyst (15 mg) in the form of a self-supported wafer; the gases leaving the cell were analyzed by a mass spectrometer (ThermoStar TM GSD 301, Pfeiffer Vacuum) and a chemiluminescence analyzer (42i-HL MEGATEC, Thermo Fisher Scientific, Waltham, MA, USA). Total flow was 25 cm$^3 \cdot$ min^{-1} (at 1 atm and 0 °C). Surface FT-IR spectra were collected with a FT-IR Nicolet Nexus spectrometer (Thermo Fisher Scientific) with 4 cm^{-1} spectral resolution and accumulation of 64 scans using a deuterated-triglycine sulfate (DTGS) detector.

The same apparatus was used to perform temperature programmed surface reaction (H$_2$- and NH$_3$-TPSR) experiments. In this case the catalysts were at first saturated with NO_x species at 350 °C by feeding NO (1000 ppm) in O$_2$ (3% *v/v*) + Ar. This resulted in the formation of surface nitrate species. Then the catalyst was cooled under He at 40 °C and subsequently heated in flowing H$_2$ (2000 ppm in

Ar, H_2-TPSR) or NH_3 (1000 ppm in Ar, NH_3-TPSR) up to 400 °C (heating rate 4 °C/min). Notably, due to the low reductant concentration, experiments were carried out under nearly isothermal conditions, *i.e.,* in the absence of significant temperature effects during the experiments. Further details concerning apparatuses and procedures can be found in [10,15].

Since the fresh catalyst samples were covered by carbonate species, before the experiments few adsorption-reduction cycles under isothermal conditions at 350 °C, (*i.e.*, NO/O_2 (1000 ppm NO + O_2 3%, *v/v*) and H_2 (2000 ppm)) were performed. This procedure partially replaces the originally present $BaCO_3$ species with $BaO/Ba(OH)_2$ species [20].

5. Conclusions

In this paper, mechanistic aspects involved in the formation of N_2O over Pt-BaO/Al_2O_3 and Rh-BaO/Al_2O_3 model NSR catalysts were investigated. In particular, the reactivity of both gas-phase NO and stored nitrates were investigated by using H_2 and NH_3 as reductants. Transient experiments with simultaneous gas phase and surface analysis using FT-IR spectroscopy were used to correlate the concentration of the gas-phase species with adsorbed surface species.

The data herein obtained provides clear indication of the fact that over both Rh- and Pt-BaO/Al_2O_3 catalysts, N_2O formation involves the presence of gas-phase NO. In fact under our experimental conditions no nitrous oxide formation was observed upon the reduction of the stored nitrate species. The data show that N_2O formation involves the coupling of undissociated NO molecules with N-adspecies formed upon NO dissociation onto reduced PGM sites. The reductant keeps the PGM sites in a reduced state by scavenging O-adatoms formed upon NO dissociation, the initial step of the process. However when complete dissociation of gas-phase NO occurs, N_2O formation is prevented. In fact N_2O formation is observed at temperatures where the reductants start to be active in the reduction of the PGM sites, whereas at higher temperatures, where the reductants effectively keep the PGM sites in a fully reduced state, complete dissociation of NO takes place and N_2O formation is not effective. This explains why N_2O formation is observed at low temperatures and then disappears at high temperatures.

Over both Rh- and Pt-BaO/Al_2O_3 catalysts N_2O formation is observed at lower temperatures with H_2 than with NH_3, in view of the higher reactivity of hydrogen in the reduction of the PGM sites. Also, N_2O formation occurs at lower temperatures onto Pt-containing catalyst if compared to the Rh-based sample, due to the higher reducibility of Pt *vs.* Rh.

In the absence of reducing agents, N_2O can be formed from NO provided that reduced PGM sites are present. In such a case O-adatoms formed upon NO decomposition are scavenged by NO itself leading to the formation of nitrite species so that the formation of N_2O occurs according to the stoichiometry of the NO disproportionation reaction Equation (1).

Finally, the fact that N_2O formation was not observed upon the reduction of stored nitrates with both H_2 and NH_3 is due to the slow rate of the NO release process from the stored species. This limits the NO gas-phase concentration during the reduction of the stored species thus preventing N_2O formation.

Author Contributions: The experimental study was conducted by L.K. and R.M. who were also responsible for preparation of the manuscript. The supervision during catalytic activity was provided by M.D. and L.C. The analysis and interpretation of the data was carried out by all authors in particular M.D., L.L., and P.F.

Conflicts of Interest: The authors declare no conflicts of interest.

References

1.　Forzatti, P.; Lietti, L.; Castoldi, L. Storage and Reduction of NO_x Over LNT Catalysts. *Catal. Lett.* **2015**, *145*, 483–504. [CrossRef]

2. Castoldi, L.; Bonzi, R.; Lietti, L.; Forzatti, P.; Morandi, S.; Ghiotti, G.; Dzwigaj, S. Catalytic behaviour of hybrid LNT/SCR systems: Reactivity and *in situ* FTIR study. *J. Catal.* **2011**, *282*, 128–144. [CrossRef]

3. Bártová, S.; Kočí, P.; Mráček, D.; Marek, M.; Pihl, J.A.; Choi, J.S.; Toops, T.J.; Partridge, W.P. New insights on N_2O formation pathways during lean/rich cycling of a commercial lean NO_x trap catalyst. *Catal. Today* **2014**, *231*, 145–154. [CrossRef]

4. Choi, J.S.; Partridge, W.P.; Pihl, J.A.; Kim, M.Y.; Kočí, P.; Daw, C.S. Spatiotemporal distribution of NO_x storage and impact on NH_3 and N_2O selectivities during lean/rich cycling of a Ba-based lean NO_x trap catalyst. *Catal. Today* **2012**, *184*, 20–26. [CrossRef]

5. Clayton, R.D.; Harold, M.P.; Balakotaiah, V. Performance Features of Pt/BaO Lean NO_x Trap with Hydrogen as Reductant. *AIChE J.* **2009**, *55*, 687–700. [CrossRef]

6. Dasari, P.; Muncrief, R.; Harold, M.P. Cyclic lean reduction of NO by CO in Excess H_2O on Pt-Rh/Ba/Al_2O_3: Elucidating mechanistic features and catalyst performance. *Top. Catal.* **2013**, *56*, 1922–1936. [CrossRef]

7. Kočí, P.; Bártová, Š.; Mráček, D.; Marek, M.; Choi, J.S.; Kim, M.Y.; Pihl, J.A.; Partridge, W.P. Effective Model for Prediction of N_2O and NH_3 Formation During the Regeneration of NO_x Storage Catalyst. *Top. Catal.* **2013**, *56*, 118–124. [CrossRef]

8. Kumar, A.; Harold, M.P.; Balakotaiah, V. Isotopic studies of NO_x storage and reduction on Pt/BaO/Al_2O_3 catalyst using temporal analysis of products. *J. Catal.* **2010**, *270*, 214–223. [CrossRef]

9. Mráček, D.; Kočí, P.; Choi, J.S.; Partridge, W.P. New operation strategy for driving the selectivity of NO_x reduction to N_2, NH_3 or N_2O during lean/rich cycling of a lean NO_x trap catalyst. *Appl. Catal. B* **2016**, *182*, 109–114. [CrossRef]

10. Kubiak, L.; Righini, L.; Castoldi, L.; Matarrese, R.; Forzatti, P.; Lietti, L.; Daturi, M. Mechanistic aspects of N_2O formation over Pt-based Lean NO_x Trap catalysts. *Top. Catal.* **2015**. submitted.

11. Taylor, K.C. Nitric Oxide Catalysis in Automotive Exhaust Systems. *Catal. Rev.* **1993**, *35*, 457–481. [CrossRef]

12. Konsolakis, M.; Yentekakis, I.V. The Reduction of NO by Propene over Ba-Promoted Pt/γ-Al_2O_3 Catalysts. *J. Catal.* **2001**, *198*, 142–150. [CrossRef]

13. Lietti, L.; Artioli, N.; Righini, L.; Castoldi, L.; Forzatti, P. Pathways for N_2 and N_2O Formation during the Reduction of NO_x over Pt–Ba/Al_2O_3 LNT Catalysts Investigated by Labelling Isotopic Experiments. *Ind. Eng. Chem. Res.* **2012**, *51*, 7597–7605. [CrossRef]

14. Kubiak, L.; Righini, L.; Castoldi, L.; Matarrese, R.; Forzatti, P.; Lietti, L.; Daturi, M. In-depth insights into N_2O formation over Rh-Ba/Al_2O_3 catalyst under operando FT-IR conditions and micro reactor study. Unpublished. 2016.

15. Lietti, L.; Nova, I.; Forzatti, P. Role of ammonia in the reduction by hydrogen of NO_x stored over Pt-Ba/Al_2O_3 lean NO_x trap catalysts. *J. Catal.* **2008**, *257*, 270–282. [CrossRef]

16. Castoldi, L.; Righini, L.; Matarrese, R.; Lietti, L.; Forzatti, P. Mechanistic aspects of the release and the reduction of NO_x stored on Pt–Ba/Al_2O_3. *J. Catal.* **2015**, *328*, 270–279. [CrossRef]

17. Epling, W.S.; Campbell, L.E.; Yezerets, A.; Currier, N.W.; Parks, J.E. Overview of the fundamental reactions and degradation mechanisms of NO_x storage/reduction catalysts. *Catal. Rev. Eng.* **2004**, *46*, 163–245. [CrossRef]

18. Kabin, K.S.; Muncrief, R.L.; Harold, M.P. NO_x storage and reduction on a Pt/BaO/alumina monolithic storage catalyst. *Catal. Today* **2004**, *96*, 79–89. [CrossRef]

19. Muncrief, R.L.; Kabin, K.S.; Harold, M.P. NO_x storage and reduction with propylene on Pt/BaO/alumina. *AIChE J.* **2004**, *50*, 2526–2540. [CrossRef]

20. Lietti, L.; Forzatti, P.; Nova, I.; Tronconi, E. NO_x Storage Reduction over PtBa/γ-Al_2O_3 Catalyst. *J. Catal.* **2001**, *204*, 175–191. [CrossRef]